Cell Injury, Repair, Aging, and Apoptosis

The Influence of Skeletal Muscle on the Regulation of Liver:Body Mass and Liver Regeneration

Jiansheng Huang,* Martin Glauber,*
Zhaohua Qiu,* Vered Gazit,* Dennis J. Dietzen,*
and David A. Rudnick*†

From the Departments of Pediatrics* and Developmental Biology,† Washington University School of Medicine, St. Louis, Missouri

The relationship between liver and body mass is exemplified by the precision with which the liver:body mass ratio is restored after partial hepatic resection. Nevertheless, the compartments, against which liver mass is so exquisitely regulated, currently remain undefined. In the studies reported here, we investigated the role of skeletal muscle mass in the regulation of liver:body mass ratio and liver regeneration via the analysis of myostatin-null mice, in which skeletal muscle is hypertrophied. The results showed that liver mass is comparable and liver:body mass significantly diminished in the null animals compared to age-, sex-, and strain-matched controls. In association with these findings, basal hepatic Akt signaling is decreased, and the expression of the target genes of the constitutive androstane receptor and the integrin-linked kinase are dysregulated in the myostatin-null mice. In addition, the baseline expression levels of the regulators of the G1-S phase cell cycle progression in liver are suppressed in the null mice. The initiation of liver regeneration is not impaired in the null animals, although it progresses toward the lower liver:body mass set point. The data show that skeletal muscle is not the body component against which liver mass is positively regulated, and thus they demonstrate a previously unrecognized systemic compartmental specificity for the regulation of liver:body mass ratio. *(Am J Pathol 2012, 180:575–582; DOI: 10.1016/j.ajpath.2011.10.032)*

Liver mass is regulated in specific proportion to body mass. Such regulation is well-illustrated by the precision with which the liver:body mass ratio is restored after partial hepatic resection,[1,2] and re-established after small- or large-graft-for-recipient size liver transplantation[3,4] in both clinical and experimental settings. Nevertheless, the body mass components and compartments against which liver mass is so precisely calibrated are undefined. We have previously demonstrated that the metabolic response to hepatic insufficiency regulates liver regeneration. Those studies showed that following partial hepatectomy, mice develop hypoglycemia,[5] catabolize systemic fat stores,[6] and transiently accumulate triglyceride fat in the regenerating liver.[7] We also showed that liver regeneration is impaired by dextrose supplementation,[5] by strategies that suppress hepatic fat accumulation,[7] and in fatty liver dystrophy (*fld*) mice with genetically-determined paucity of systemic adipose.[6] These findings suggest that catabolism of systemic fat stores might be essential for liver regeneration. We have also observed that extrahepatic lean tissue is catabolized after partial hepatectomy or carbon tetrachloride (CCl_4) administration,[6] and that in each case the subsequent regenerative response is associated with significant induction in skeletal muscle of mRNA encoding the muscle-specific E3 ubiquitin protein ligases MuRF1 and MafBx (D.A. Rudnick, unpublished observations).[8] Those findings raise the possibility that muscle mass could also contribute to the regulation of liver mass and regeneration. Here, we investigated whether increased skeletal muscle mass, as occurs in mice in which myostatin expression is genetically disrupted,[9,10] influences the regulation of liver:body mass or the hepatic regenerative response to partial hepatectomy.

Materials and Methods

Animal Husbandry

Myostatin-null mice were generated as previously described.[9,10] Null, heterozygous, and wild-type mice,

bred from mating pairs heterozygous for the null allele, were maintained on 12 hours dark-light cycles with *ad libitum* access to standard rodent chow and water. Three-month-old male mice were used for all experiments, except where otherwise specifically indicated. Some mice were subjected to two-thirds partial hepatectomy or sham surgery.[5,6,11,12] Three or more animals were examined at each time point for each genotype. All experiments were approved by the Animal Studies Committee at Washington University School of Medicine and conducted in accordance with the institutional guidelines and the criteria outlined in the "Guide for Care and Use of Laboratory Animals" (NIH Publication No. 86-23).

Histology and Immunohistochemistry

Animals were given an intraperitoneal injection of 100 mg/kg 5-bromo-2′-deoxyuridine (BrdU) 1 hour before sacrifice. Formalin-fixed, paraffin-embedded liver tissue was stained with H&E for nuclear BrdU incorporation or for TUNEL. Hepatocellular nuclear BrdU labeling and mitoses were quantified by examining at least three random ×400 fields and at least 300 cells and nuclei in each tissue section.[5,6,12,13] TUNEL staining was performed with the In Situ Cell-Death Detection Kit (Roche, Mannheim, Germany) with DAPI as nuclear counterstain, according to the manufacturer's instructions. Hepatocellular apoptosis was quantified as the percentage of TUNEL-positive cells in 10 to 20 high-powered (×400) fields using a fluorescent microscope (AxioVision, Zeiss, Thronwood, NY). A TUNEL positive control was generated by pretreatment with DNase I, according to the manufacturer's instructions.

Gene Expression Analysis

Expression levels of specific genes of interest were determined by semiquantitative, RT-qPCR as described previously.[5–7,12–14] Briefly, total liver RNA was extracted using TRIzol (Invitrogen, Carlsbad, CA) and was reverse transcribed to cDNA. An aliquot of cDNA was added to a reaction mixture containing gene-specific forward and reverse primers, deoxynucleotides, TaqDNA polymerase, and SYBR Green (Stratagene, La Jolla, CA). Primers were identified from the literature or using Primer Bank software (http://pga.mgh.harvard.edu/primerbank/). Quantification of mRNA expression was based on monitoring increased SYBR Green fluorescence during exponential phase amplification in a real-time PCR MxPro3005 Machine (Stratagene) using the comparative threshold (Ct) method.[15] The data were standardized to the expression of β2-microglobulin.[16–19] Specificity was verified for each gene by confirmation of predicted product size and uniformity using melt-curves and agarose-gel electrophoresis of the PCR products, and by simultaneous analysis of a reaction mixture containing all components except reverse transcriptase. Primers used for these analyses included: Alb (albumin): forward 5′-TTGCCGATGAGTCTGCCGCC-3′, reverse 5′-GGAGGTGCACATGGCCTCAGC-3′; Axin2: for-

ward 5′-TGACTCTCCTTC-CAGATCCCA-3′, reverse 5′-TGCCCACACTAGGCTGACA-3′; β2-microglobulin: forward 5′-TGGCTGCTTCTTTCGATTTCTG-3′, reverse 5′-CCA-GAAAACCCCTCAAATTCAAG-3′; Car: forward 5′-GC-CACTGTCCAGCCTGCAGG-3′, reverse 5′-TTTCTCTGC-CCGCCGCTGTG-3′; Cdc25A: forward 5′-TCTGCACA-TGGAAGAAGAGG-3′, reverse 5′-TTGCCATCAGTAGG-CACAAT-3′; Cyclin D1: forward 5′-GAAGGAGACCAT-TCCCTTGA-3′, reverse 5′-GTTCACCAGAAGCAGTTC-CA-3′; Cyclin E: forward 5′-CTCGGGTGTTGTAGGT-TGCT-3′, reverse 5′-CTGTTGGCTGACAGTGGAGA-3′; Cyp2b10: forward 5′-TCCCCTGCCCCTCTTGGGGA-3′, reverse 5′-CAGGCCTTGGTCCCAGGTGC-3′; Cyp3a11: forward 5′-TGGAAACCTGGGTGCTCCTAGCA-3′, reverse 5′-GGCAGAGGTTTGGGCCCAGG-3′; fructose bisphosphatase 1 (Fbp1): forward 5′-TCTGTTTCGATC-CCCTTGAT-3′, reverse 5′-GCTGCAGAGCATCCTTCTC-3′; and Ilk: forward 5′-GGTGCGCTTGTGGCTGGACA-3′, reverse 5′-CACCGCAGAGCGGCCTTCTC-3′.

Protein Expression

Proteins were quantified in whole tissue lysates, as previously described.[5,6,12,13] Briefly, lysates were subjected to SDS-PAGE, followed by electrophoretic transfer to nitrocellulose membrane. The filters were probed with primary antibodies specific for each of the analyzed proteins (total Akt, Ser 473 phospho-Akt, GSK3β, Ser 9 phospho-GSK3β, S6 kinase, Thr 421/Ser 424 phospho-S6 kinase, β-catenin, and Ser 127 phospho-YAP (Cell Signaling, Beverly, MA); glyceraldehydes-3-phosphate dehydrogenase (GAPDH, Chemicon/Millipore, Temecula, CA); total YAP (Santa Cruz Biotechnology, Santa Cruz, Ca) followed by appropriate infrared fluorophore-conjugated secondary antibodies (Li-COR Biosciences, Lincoln, NE). Reactivity was quantified using the Odyssey Infrared Imaging System (Li-COR Biosciences, Lincoln, NE).

Transaminase Measurement

Tissue alanine aminotransferase activity was determined using a lactate dehydrogenase coupled assay supplemented with pyridoxal phosphate on the Cobas c501 chemistry system (Roche Diagnostics, Indianapolis, IN).

Statistical Analysis

Data were analyzed using SigmaPlot version 8.02, SigmaStat version 3, and PASW Statistics version 18.0 (SPSS, Chicago, IL). Unpaired Student's *t*-test for pairwise comparisons and analysis of variance for multiple groups were used with significance (α) set at 0.05. Data are reported as mean $\pm$ SE.
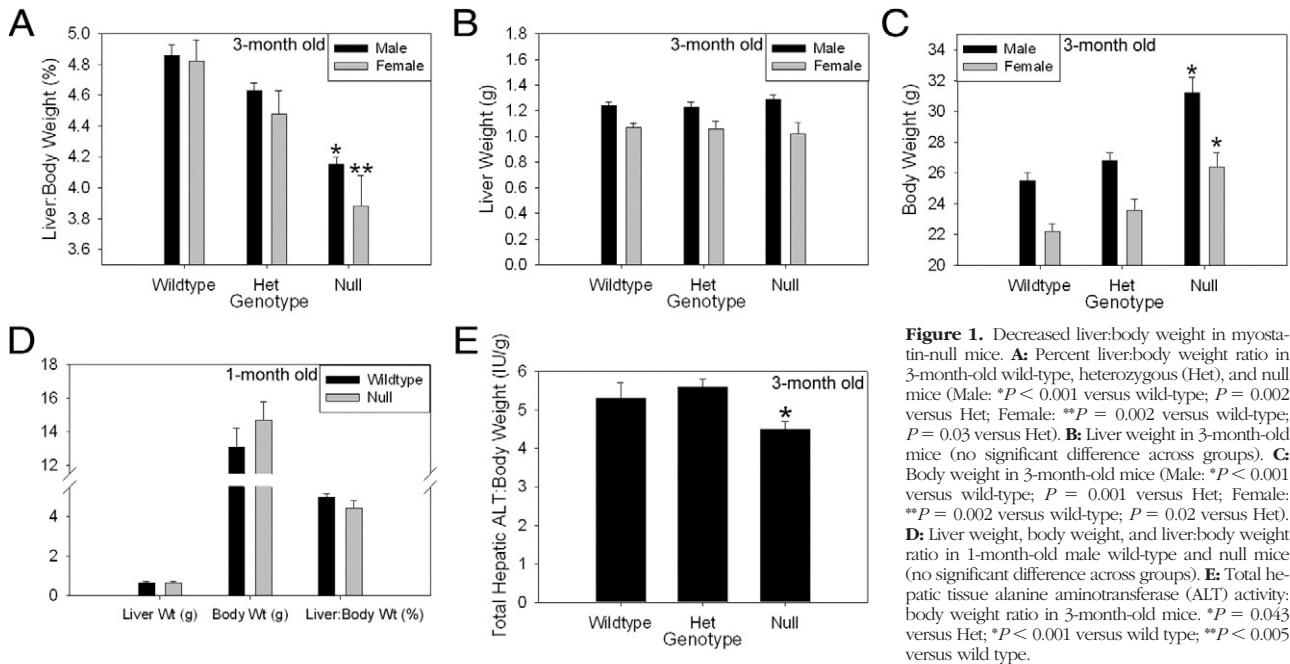
Figure 1. Decreased liver:body weight in myostatin-null mice. **A:** Percent liver:body weight ratio in 3-month-old wild-type, heterozygous (Het), and null mice (Male: *$P < 0.001$ versus wild-type; $P = 0.002$ versus Het; Female: **$P = 0.002$ versus wild-type; $P = 0.03$ versus Het). **B:** Liver weight in 3-month-old mice (no significant difference across groups). **C:** Body weight in 3-month-old mice (Male: *$P < 0.001$ versus wild-type; $P = 0.001$ versus Het; Female: **$P = 0.002$ versus wild-type; $P = 0.02$ versus Het). **D:** Liver weight, body weight, and liver:body weight ratio in 1-month-old male wild-type and null mice (no significant difference across groups). **E:** Total hepatic tissue alanine aminotransferase (ALT) activity: body weight ratio in 3-month-old mice. *$P = 0.043$ versus Het; *$P < 0.001$ versus wild type; **$P < 0.005$ versus wild type.

Results

Liver Mass Is Not Increased, and the Liver:Body Mass Ratio Is Reduced in Myostatin-Null Mice

First, we compared the liver:body mass ratio in 3-month-old myostatin-null mice to that observed in strain-, age-, and sex-matched wild-type and heterozygous control animals. Myostatin is a transforming growth factor-β-superfamily member that negatively regulates muscle mass, and myostatin-null mice have increased skeletal muscle.[9,10] Surprisingly, despite significantly greater muscle mass, and therefore total body mass, in myostatin-null mice compared to control animals, absolute liver weight is comparable and the liver:body mass ratio is significantly lower in the null mice (Figure 1, A–C). These data indicate that liver mass and the liver:body mass ratio are not increased in proportion to skeletal muscle mass in adult mice. To assess for developmental effects on liver:body mass regulation in these animals, 1-month-old male myostatin null mice were also examined. These younger mice also showed a higher body mass and lower liver:body mass ratio compared to controls; however, the differences were not as great as those seen in the older animals and did not reach statistical significance (Figure 1D; $P = 0.15$). These data indicate that the difference in liver:body mass ratio between adult myostatin null mice and controls develops as muscle mass increases in the null animals. In an effort to assess whether liver function in proportion to body mass is also reduced in myostatin null mice, we quantified total liver tissue transaminase activity in adult null and control mice. Previously we reported that the magnitude of such tissue activity is proportionate to liver mass.[20] Similar analysis here showed comparable total hepatic alanine transaminase activity (data not shown) and a lower total hepatic tissue alanine aminotransferase activity to body mass ratio in null versus control animals (Figure 1E). These data show that liver function assessed by this measure, as with liver mass, is reduced relative to body mass in myostatin-null mice.

Hepatic Akt Activation Is Decreased in Myostatin-Null Mice

The previously described data show that the liver:body mass set point (ie, the "hepatostat"[2]) is lower in adult myostatin-null mice than in age-, sex-, and strain-matched control animals. One possible explanation for this observation is that another body mass compartment against which liver mass is regulated is also unchanged in the myostatin-null mice. For example, systemic fat mass has been reported to be comparable between young adult myostatin-null mice and matched controls,[9] and our previous studies implicate peripheral adipose stores as an important determinant of normal liver regeneration.[6,7] Alternatively, decreased liver:body weight ratio in myostatin-null mice could be the result of signals generated by or in response to increased muscle mass. The observation that myostatin-null mice exhibit increased insulin sensitivity and correspondingly decreased levels of circulating insulin[21] suggests that activation of the insulin-responsive Akt signaling pathway might be suppressed in myostatin-null mice. Activation of this pathway is known to increase liver mass[22] and regulate liver regeneration.[23,24] Based on this consideration, we compared basal hepatic Akt-dependent signaling between myostatin-null and control mice. The results showed that the level of activated (serine 473 phosphorylated) hepatic Akt is significantly lower in null mice than in controls (Figure 2, A and B). Phosphorylation of GSK3β, which is a downstream target of the Akt kinase, is also decreased in myostatin-null mouse liver compared to controls, whereas that of S6 kinase, another Akt target,
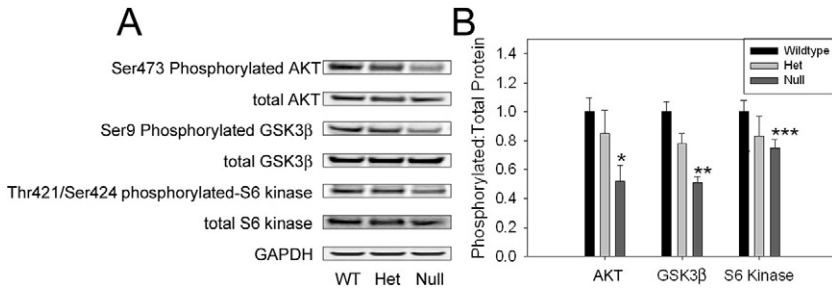
Figure 2. Decreased hepatic AKT pathway activation in myostatin-null mice. Representative protein immunoblot (**A**) and quantitative summary of basal hepatic expression (**B**) of Ser 473 phosphorylated- and total AKT, Ser 9 phosphorylated- and total GSK3β, and Thr 421/Ser 424 phosphorylated- and total S6 kinase standardized to glyceraldehydes-3-phosphate dehydrogenase (GAPDH) loading control in 3-month-old wild-type (WT), heterozygous (Het), and myostatin-null mice. GAPDH is shown as loading control. *$P = 0.02$ versus wild type; **$P < 0.001$ versus wild type; $P = 0.02$ versus Het; ***$P = 0.09$ versus wild type.

appears reduced but the differences are not significant (Figure 2, A and B). These findings show that the basal level of Akt pathway activation is reduced in myostatin-null mouse liver.

Comparison of Signals Implicated in Liver:Body Mass Regulation between Myostatin-Null and Control Mice

In addition to Akt, a number of other molecular pathways have been implicated in the regulation of liver mass. For example, pharmacological activation of the constitutive androstane receptor (CAR)[25,26] and genetic induction of β-catenin signaling[27–30] promote increased liver mass. Inactivation of the MST1/2 (Hippo) kinase cascade[31] and deletion of the integrin-linked kinase (ILK)[32] also increase liver mass. Therefore, we compared the activation state and the expression of key components of each of these pathways in livers from myostatin-null and control mice.

First, the β-catenin pathway was assessed. The results showed comparable hepatic expression of β-catenin protein (Figure 3A) and of the β-catenin-target gene Axin2 (Figure 3B) in control and null mice. Analysis of the Hippo kinase pathway also showed no effect of myostatin deficiency on hepatic levels of the downstream target of this cascade, (Ser 127) phosphorylated Yes association protein (YAP) (p-YAP, Figure 3C). p-YAP mediates the inhibitory effect of the mammalian Hippo ortholog MST1/2 on liver size.[33] Next, CAR signaling was examined. Expression of the CAR target gene Cyp2b10 is significantly decreased in the nulls (Figure 3D). Car mRNA expression is also modestly reduced in these animals, but this difference is not significant (Figure 3D) ($P = 0.1$ versus wild type). Hepatic expression of Ilk is significantly reduced in the myostatin-null mice, and surprisingly mRNA expression of Cyp3a11, which is negatively regulated by ILK,[32] is also reduced in the nulls (Figure 3D). Similarly, Albumin and Fbp1 mRNA expression, which are also suppressed
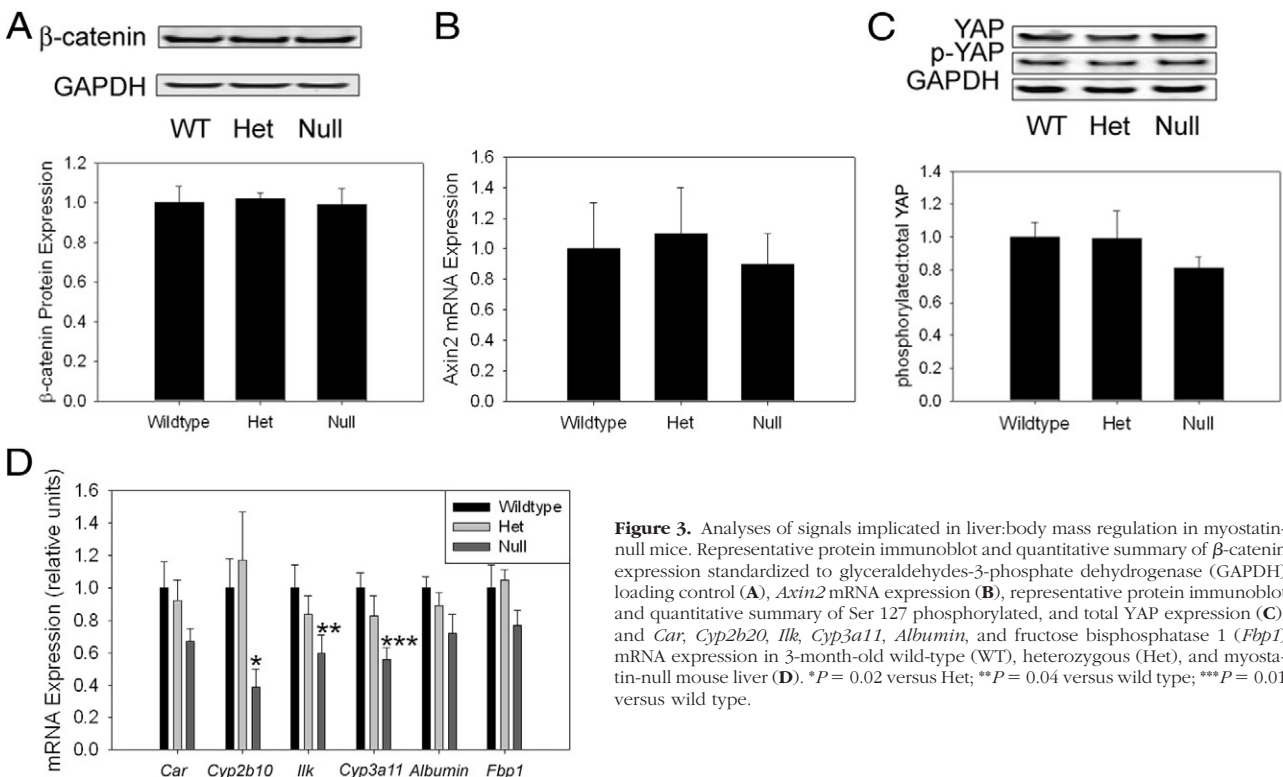

Figure 3. Analyses of signals implicated in liver:body mass regulation in myostatin-null mice. Representative protein immunoblot and quantitative summary of β-catenin expression standardized to glyceraldehydes-3-phosphate dehydrogenase (GAPDH) loading control (**A**), *Axin2* mRNA expression (**B**), representative protein immunoblot and quantitative summary of Ser 127 phosphorylated, and total YAP expression (**C**), and *Car*, *Cyp2b20*, *Ilk*, *Cyp3a11*, *Albumin*, and fructose bisphosphatase 1 (*Fbp1*) mRNA expression in 3-month-old wild-type (WT), heterozygous (Het), and myostatin-null mouse liver (**D**). *$P = 0.02$ versus Het; **$P = 0.04$ versus wild type; ***$P = 0.01$ versus wild type.
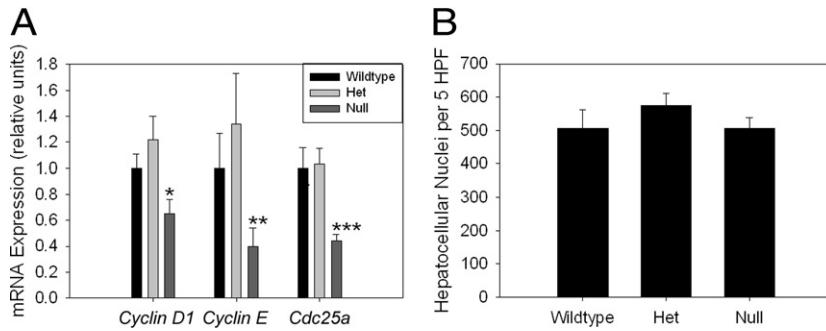
Figure 4. Hepatic expression of cell cycle regulators and determination of hepatocellular size in myostatin-null mice. Basal hepatic *Cyclin D1, Cyclin E,* and *Cdc25A* mRNA expression (**A**) and hepatocellular nuclear density (number of nuclei per five ×400 high-powered-fields [HPF], as a surrogate for hepatocyte size) (**B**) in 3-month-old wild-type, heterozygous, and myostatin-null mice. *$P = 0.1$ versus wild type; $P = 0.02$ versus Het; **$P = 0.2$ versus wild type; $P = 0.05$ versus Het; ***$P = 0.01$ versus wild type, Het.

by ILK,[32] are modestly (but not significantly) reduced in the myostatin knockouts (Figure 3D). These observations demonstrate discordance between the regulation of ILK expression and activity in myostatin-null mice, and more importantly that basal hepatic ILK activity appears to be increased in these animals (based on the diminished expression of genes negatively regulated by ILK,[32]). Taken together, these findings suggest that changes in hepatic CAR or ILK activity contribute to the observed alteration of the "hepatostat" in myostatin-null mice.

Regulators of G1-S Phase Cell Cycle Progression Exhibit Reduced Expression in Myostatin-Null Mice

Akt-, CAR-, and ILK-dependent signaling pathways might influence liver:body mass through effects on proliferation, size, or survival of liver cells; therefore, these parameters were investigated in the livers of myostatin-null and control mice. We observed no detectable hepatocellular BrdU incorporation or mitosis in control mice at baseline (data not shown); thus, any inhibitory effect of myostatin deficiency on hepatocellular proliferation is not demonstrable using this approach. Cyclin D1 regulates cellular proliferation and cell size,[34] and its expression is regulated by Akt[34] and CAR[26] activation. Therefore, we determined hepatic expression of Cyclin D1 mRNA in myostatin-null and control mice, with the results showing significantly lower levels in the null mice (Figure 4A). mRNA abundances of Cyclin E and Cdc25A, which also regulate G1-S progression, are lower in null animals as

well (Figure 4A). Next, we estimated hepatocyte cell size by hepatocellular nuclear density,[35] and found no difference between null mice and controls (Figure 4B). Finally, we investigated effects on cell survival by assessment of hepatocellular apoptosis. Again, we observed no difference in the very low basal rate of hepatocellular apoptosis in livers from myostatin-null and control animals (Figure 5). These data indicate that decreased liver:body mass is associated with lower expression of Cyclin D1, Cyclin E, and Cdc25A, which could result from decreased basal activation of insulin-dependent hepatic Akt signaling or CAR in myostatin-null mice. These data also show that hepatocellular size and apoptosis are not altered in the null animals.

Liver Regeneration in Response to Partial Hepatectomy Is Normally Induced in Myostatin-Null Mice

Activation of Akt and increased expression of Cyclin D1, Cyclin E, and Cdc25A occur during the hepatic regenerative response to partial hepatectomy.[23,34] Therefore, based on the results previously described, we compared liver regeneration in myostatin-null and control mice next. Analyses of hepatocellular proliferation showed comparable hepatocellular BrdU incorporation 36 hours after partial hepatectomy (the time of peak proliferation in wild-type mice) in null and control animals (Figure 6, A and B). Similarly, hepatocellular mitotic frequency 48 hours after surgery (the time of peak mitotic progression during normal regeneration) is not affected in the null mice (Figure 6, A and B). We also assessed recovery of liver mass
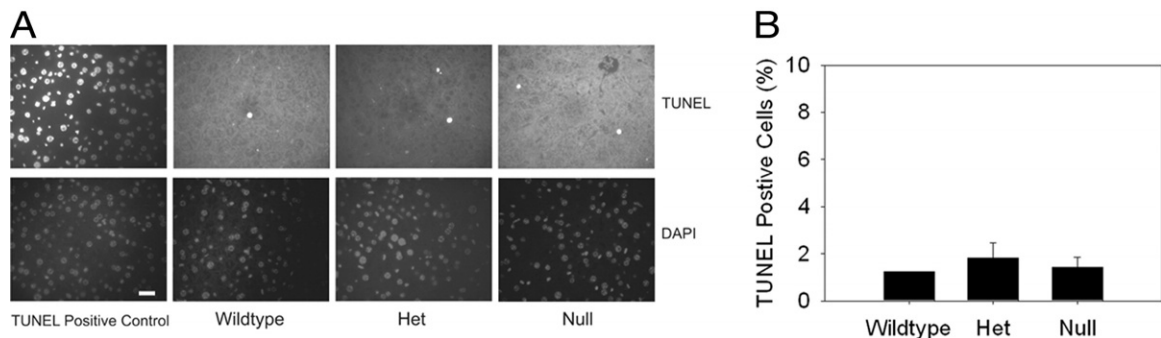

Figure 5. Hepatocellular apoptosis in myostatin-null mice. Representative TUNEL and DAPI-stained liver sections (**A**) and quantitative summary of TUNEL-positive cells (**B**) in liver sections from 3-month-old wild-type, heterozygous (Het), and myostatin-null mice (20 micron bar shown in DAPI-stained TUNEL positive control liver section; no significant difference across groups).
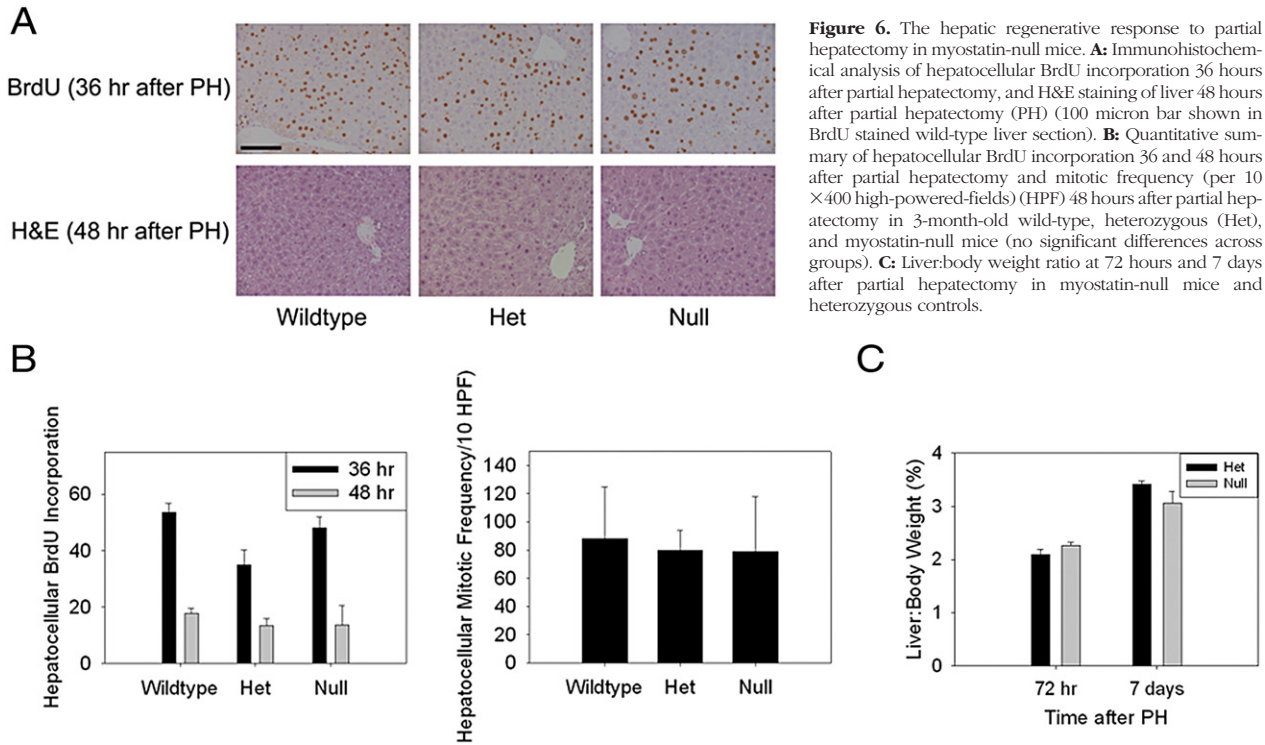
A

BrdU (36 hr after PH)

H&E (48 hr after PH)

Wildtype   Het   Null

B

C

Figure 6. The hepatic regenerative response to partial hepatectomy in myostatin-null mice. **A:** Immunohistochemical analysis of hepatocellular BrdU incorporation 36 hours after partial hepatectomy, and H&E staining of liver 48 hours after partial hepatectomy (PH) (100 micron bar shown in BrdU stained wild-type liver section). **B:** Quantitative summary of hepatocellular BrdU incorporation 36 and 48 hours after partial hepatectomy and mitotic frequency (per 10 ×400 high-powered-fields) (HPF) 48 hours after partial hepatectomy in 3-month-old wild-type, heterozygous (Het), and myostatin-null mice (no significant differences across groups). **C:** Liver:body weight ratio at 72 hours and 7 days after partial hepatectomy in myostatin-null mice and heterozygous controls.

after partial hepatic resection. The results showed that the liver:body weight ratio is lower in myostatin-null mice compared to controls 7 days after the surgery; however, this difference did not reach statistical significance (Figure 6C) ($P = 0.1$). These findings indicate that induction of liver regeneration is not suppressed in myostatin-null mice, and therefore that the initiation of the regenerative response is not proportionate to the liver:body mass ratio. The data also suggest that regeneration proceeds toward the lower liver:body weight set point in the myostatin-null mice.

Discussion

Experimental analyses of liver regeneration portray the precision with which liver:body mass is regulated. The most robust support for this concept comes from the rodent partial hepatectomy model, in which regeneration is directly proportional to the magnitude of hepatic injury,[6] and the pre-hepatectomy liver:body mass ratio is restored before termination of regeneration.[1,2] Additional evidence of this precise control comes from studies of experimental and clinical liver transplantation, in which small-for-recipient-size grafts enlarge and large organs become smaller after transplantation, until the appropriate liver:body mass ratio is ultimately attained.[3,4] Finally, analyses of mitogen-induced hepatomegaly show that withdrawal of the mitogenic stimulus is also followed by restoration of the liver:body mass set point.[36] Nevertheless, the molecular mechanisms that regulate this putative "hepatostat" continue to be sought.[2] Elucidation of this regulation requires not only the characterization of the intrahepatic signaling events involved, but also determination of the

body mass compartments against which liver mass is so precisely maintained.

We have previously reported data demonstrating the functional importance of the metabolic response to hepatic insufficiency during experimental liver regeneration.[5–7,13] Those studies implicated catabolism of adipose as essential for normal liver regeneration,[6] but did not establish if that requirement is based on adipose stores as a source of metabolic fuel to support regeneration, lipid precursor for new membrane synthesis, a specific signal that initiates the regenerative response itself, or, perhaps, all of these. Our investigations also demonstrated catabolism of systemic lean stores[6] and induction of the muscle-specific E3 ubiquitin ligases, MuRF1 and MafBx, in both the partial hepatectomy and carbon tetrachloride models of liver regeneration (D.A. Rudnick, unpublished data[8]). Here, we extend on this work by investigating the influence of skeletal muscle on liver:body mass regulation and liver regeneration. Surprisingly, liver mass is unchanged and liver:body mass is significantly reduced in myostatin-null animals, which exhibit significant skeletal muscle hypertrophy.[9,10] This finding indicates that the liver:body mass ratio set point (ie, the "hepatostat") is reduced in myostatin-null mice, a conclusion supported by the diminished liver:body weight ratio that we observed 1 week after partial hepatectomy in these mice (Figure 6C).

We investigated several possible mechanisms to explain decreased liver:body mass in myostatin knockout animals. Because these mice exhibit increased insulin sensitivity and correspondingly diminished circulating levels of insulin,[21] we first examined the insulin sensitive Akt pathway. Our finding that the myostatin-null mice

display decreased basal hepatic activation of this pathway, together with published data showing that Akt signaling regulates liver mass and liver regeneration,[22–24] suggest that differences in Akt pathway activity likely contribute to the decreased liver:body mass ratio in these animals. Our investigations did not identify differences between null and control mice in either the β-catenin or Hippo kinase pathways. Each of these signaling cascades also influences liver:body mass regulation,[27–31] and recent analyses show that Hippo regulates β-catenin signaling.[37] In contrast, both CAR and ILK signaling appear to be dysregulated in the myostatin-null mouse liver, and interestingly these pathways have also been reported to interact.[38] These findings, together with our data showing myostatin deficiency, does not impact hepatocyte size or hepatocellular apoptosis, suggest that the reduced liver:body mass in these animals is secondary to diminished basal hepatocellular proliferation. We did not observe decreased proliferation directly because basal rates of hepatocellular BrdU incorporation and mitosis are undetectable in the wild-type controls in these experiments (data not shown). However, hepatic expression of cyclin D1 and other regulators of cell cycle progression are significantly reduced in the myostatin-null mice compared to controls. Because expression of cyclin D1 by itself is sufficient to induce hepatocellular proliferation and increase liver size,[39] the changes observed here suggest a cyclin D1-dependent mechanism to explain the observed liver:body mass phenotype. Moreover, previously published data showing that Akt induces cyclin D1 expression suggests that reduced hepatic Akt activation is responsible for diminished cyclin D1 expression in these animals; however, it is important to note that the data reported here do not directly demonstrate this causal relationship.

As previously noted, our data demonstrate that absolute liver mass is comparable (and liver:body mass reduced) in juvenile and adult, sex-matched myostatin-null and control mice. This finding, together with the significant increase in muscle mass, and thus total body mass, in myostatin-null mice, accounts for the decreased liver:body mass ratio in these animals. This observation poses the following question: Is liver mass suppressed (below the strain-defined "ideal" liver:body mass ratio) by increased muscle mass, perhaps through the effects of such increase on insulin sensitivity and Akt signaling, hepatic ILK, and CAR activity, and expression of cell cycle regulators? Alternatively, is the (as-yet undefined) body compartment, against which liver mass and perhaps hepatic β-catenin expression and Hippo kinase pathway signaling are normally regulated, also unchanged in myostatin-null mice? It is intriguing to note that young adult myostatin-null mice, which were studied here, exhibit comparable amounts of body fat mass compared to their strain matched wild-type counterparts,[9] but as these animals age (or if they are made leptin-deficient) they accumulate less fat than their myostatin-expressing counterparts.[40] Thus, the data reported here provide additional, albeit indirect, evidence in support of the previously suggested role for systemic adiposity in the regulation of liver:body mass and liver regeneration[6,7,41,42]

(ie, the liver mass:fat mass ratio appears to be preserved in myostatin-null animals). Although another, unidentified compartment against which liver mass is regulated may also be unaffected in myostatin nulls, the data we present here establish that skeletal muscle is not the body site against which liver mass is positively regulated during development or restored by regeneration following injury. Thus, these findings demonstrate a previously unrecognized systemic compartmental specificity that must exist in liver:body mass regulation, and should prompt future interrogation of sites other than skeletal muscle as the master calibrator of hepatic size.

Acknowledgments

References

1. Michalopoulos GK: Liver regeneration. J Cell Physiol 2007, 213:286–300
2. Michalopoulos GK: Liver regeneration after partial hepatectomy: critical analysis of mechanistic dilemmas. Am J Pathol 2010, 176:2–13
3. Kam I, Lynch S, Svanas G, Todo S, Polimeno L, Francavilla A, Penkrot RJ, Takaya S, Ericzon BG, Starzl TE, Van Thiel DH: Evidence that host size determines liver size: studies in dogs receiving orthotopic liver transplants. Hepatology 1987, 7:362–366
4. Van Thiel DH, Gavaler JS, Kam I, Francavilla A, Polimeno L, Schade RR, Smith J, Diven W, Penkrot RJ, Starzl TE: Rapid growth of an intact human liver transplanted into a recipient larger than the donor. Gastroenterology 1987, 93:1414–1419
5. Weymann A, Hartman E, Gazit V, Wang C, Glauber M, Turmelle Y, Rudnick DA: p21 is required for dextrose-mediated inhibition of mouse liver regeneration. Hepatology 2009, 50:207–215
6. Gazit V, Weymann A, Hartman E, Finck BN, Hruz PW, Tzekov R, Rudnick DA: Liver regeneration is impaired in lipodystrophic fatty liver dystrophy mice. Hepatology 2010, 52:2109–2117
7. Shteyer E, Liao Y, Muglia LJ, Hruz PW, Rudnick DA: Disruption of hepatic adipogenesis is associated with impaired liver regeneration in mice. Hepatology 2004, 40:1322–1332
8. Bodine SC, Latres E, Baumhueter S, Lai VK, Nunez L, Clarke BA, Poueymirou WT, Panaro FJ, Na E, Dharmarajan K, Pan ZQ, Valenzuela DM, DeChiara TM, Stitt TN, Yancopoulos GD, Glass DJ: Identification of ubiquitin ligases required for skeletal muscle atrophy. Science 2001, 294:1704–1708
9. McPherron AC, Lawler AM, Lee SJ: Regulation of skeletal muscle mass in mice by a new TGF-beta superfamily member. Nature 1997, 387:83–90
10. Lee SJ: Regulation of muscle mass by myostatin. Annu Rev Cell Dev Biol 2004, 20:61–86
11. Rudnick DA, Dietzen DJ, Turmelle YP, Shepherd R, Zhang S, Belle SH, Squires R, the Pediatric Acute Liver Failure Study Group: Serum alpha-NH-butyric acid may predict spontaneous survival in pediatric acute liver failure. Pediatr Transplant 2009, 13: 223–230
12. Clark A, Weymann A, Hartman E, Turmelle Y, Carroll M, Thurman JM, Holers VM, Hourcade DE, Rudnick DA: Evidence for non-traditional activation of complement factor C3 during murine liver regeneration. Mol Immunol 2008, 45:3125–3132
13. Turmelle YP, Shikapwashya O, Tu S, Hruz PW, Yan Q, Rudnick DA: Rosiglitazone Inhibits Mouse Liver Regeneration. The FASEB J 2006, 20:2609–2611

14. Rudnick DA, Shikapwashya O, Blomenkamp K, Teckman JH: Indomethacin increases liver damage in a murine model of liver injury from alpha-1-antitrypsin deficiency. Hepatology 2006, 44:976–982

15. Schefe JH, Lehmann KE, Buschmann IR, Unger T, Funke-Kaiser H: Quantitative real-time RT-PCR data analysis: current concepts and the novel "gene expression's CT difference" formula. J Mol Med 2006, 84:901–910

16. Cressman DE, Greenbaum LE, DeAngelis RA, Ciliberto G, Furth EE, Poli V, Taub R: Liver failure and defective hepatocyte regeneration in interleukin-6- deficient mice. Science 1996, 274:1379–1383

17. Yamada Y, Kirillova I, Peschon JJ, Fausto N: Initiation of liver growth by tumor necrosis factor: deficient liver regeneration in mice lacking type I tumor necrosis factor receptor. Proc Natl Acad Sci U S A 1997, 94:1441–1446

18. Yamada Y, Webber EM, Kirillova I, Peschon JJ, Fausto N: Analysis of liver regeneration in mice lacking type 1 or type 2 tumor necrosis factor receptor: requirement for type 1 but not type 2 receptor. Hepatology 1998, 28:959–970

19. Greenbaum LE, Li W, Cressman DE, Peng Y, Ciliberto G, Poli V, Taub R: CCAAT enhancer- binding protein beta is required for normal hepatocyte proliferation in mice after partial hepatectomy. J Clin Invest 1998, 102:996–1007

20. Qiu Z, Longshore SW, Warner BW, Rudnick DA: Murine functional liver mass is reduced following partial small bowel resection. J Gastrointest Surg 2009, 13:2176–2182

21. Wilkes JJ, Lloyd DJ, Gekakis N: Loss-of-function mutation in myostatin reduces tumor necrosis factor alpha production and protects liver against obesity-induced insulin resistance. Diabetes 2009, 58:1133–1143

22. Mullany LK, Nelsen CJ, Hanse EA, Goggin MM, Anttila CK, Peterson M, Bitterman PB, Raghavan A, Crary GS, Albrecht JH: Akt-mediated liver growth promotes induction of cyclin E through a novel translational mechanism and a p21-mediated cell cycle arrest. J Biol Chem 2007, 282:21244–21252

23. Haga S, Ozaki M, Inoue H, Okamoto Y, Ogawa W, Takeda K, Akira S, Todo S: The survival pathways phosphatidylinositol-3 kinase (PI3-K)/phosphoinositide-dependent protein kinase 1 (PDK1)/Akt modulate liver regeneration through hepatocyte size rather than proliferation. Hepatology 2009, 49:204–214

24. Haga S, Ogawa W, Inoue H, Terui K, Ogino T, Igarashi R, Takeda K, Akira S, Enosawa S, Furukawa H, Todo S, Ozaki M: Compensatory recovery of liver mass by Akt-mediated hepatocellular hypertrophy in liver-specific STAT3-deficient mice. J Hepatol 2005, 43:799–807

25. Locker J, Tian J, Carver R, Concas D, Cossu C, Ledda-Columbano GM, Columbano A: A common set of immediate-early response genes in liver regeneration and hyperplasia. Hepatology 2003, 38:314–325

26. Columbano A, Ledda-Columbano GM, Pibiri M, Cossu C, Menegazzi M, Moore DD, Huang W, Tian J, Locker J: Gadd45beta is induced through a CAR-dependent, TNF-independent pathway in murine liver hyperplasia. Hepatology 2005, 42:1118–1126

27. Tan X, Apte U, Micsenyi A, Kotsagrelos E, Luo JH, Ranganathan S, Monga DK, Bell A, Michalopoulos GK, Monga SP: Epidermal growth factor receptor: a novel target of the Wnt/beta-catenin pathway in liver. Gastroenterology 2005, 129:285–302

28. Tan X, Behari J, Cieply B, Michalopoulos GK, Monga SP: Conditional deletion of beta-catenin reveals its role in liver growth and regeneration. Gastroenterology 2006, 131:1561–1572

29. Sekine S, Gutierrez PJ, Lan BY, Feng S, Hebrok M: Liver-specific loss of beta-catenin results in delayed hepatocyte proliferation after partial hepatectomy. Hepatology 2007, 45:361–368

30. Thompson MD, Monga SP: WNT/beta-catenin signaling in liver health and disease. Hepatology 2007, 45:1298–1305

31. Dong J, Feldmann G, Huang J, Wu S, Zhang N, Comerford SA, Gayyed MF, Anders RA, Maitra A, Pan D: Elucidation of a universal size-control mechanism in Drosophila and mammals. Cell 2007, 130:1120–1133

32. Gkretsi V, Apte U, Mars WM, Bowen WC, Luo JH, Yang Y, Yu YP, Orr A, St Arnaud R, Dedhar S, Kaestner KH, Wu C, Michalopoulos GK: Liver-specific ablation of integrin-linked kinase in mice results in abnormal histology, enhanced cell proliferation, and hepatomegaly. Hepatology 2008, 48:1932–1941

33. Song H, Mak KK, Topol L, Yun K, Hu J, Garrett L, Chen Y, Park O, Chang J, Simpson RM, Wang CY, Gao B, Jiang J, Yang Y: Mammalian Mst1 and Mst2 kinases play essential roles in organ size control and tumor suppression. Proc Natl Acad Sci U S A 2010, 107:1431–1436

34. Nelsen CJ, Rickheim DG, Tucker MM, Hansen LK, Albrecht JH: Evidence that cyclin D1 mediates both growth and proliferation downstream of TOR in hepatocytes. J Biol Chem 2003, 278:3656–3663

35. Miguel PO, Hernandez-Blasquez J, de Sousa e Silva RA, da Silva JR, Peduto L, Maltauro SM, Abrao SW, Abrao SW Jr.: Reduction of liver mass due to malnutrition in rats. Correlation with emaciation of animals and size of organs not inserted in the portal system. Sao Paulo Med J 1995, 113:903–909

36. Columbano A, Shinozuka H: Liver regeneration versus direct hyperplasia. The FASEB J 1996, 10:1118–1128

37. Varelas X, Miller BW, Sopko R, Song S, Gregorieff A, Fellouse FA, Sakuma R, Pawson T, Hunziker W, McNeill H, Wrana JL, Attisano L: The Hippo pathway regulates Wnt/beta-catenin signaling. Dev Cell 2010, 18:579–591

38. Donthamsetty S, Bhave VS, Kliment CS, Bowen WC, Mars WM, Bell AW, Stewart RE, Orr A, Wu C, Michalopoulos GK: Excessive hepatomegaly of mice with hepatocyte-targeted elimination of integrin linked kinase following treatment with 1,4-bis [2-(3,5-dichaloropyridyloxy)] benzene. Hepatology 2011, 53:587–595

39. Nelsen CJ, Rickheim DG, Timchenko NA, Stanley MW, Albrecht JH: Transient expression of cyclin D1 is sufficient to promote hepatocyte replication and liver growth in vivo. Cancer Res 2001, 61:8564–8568

40. McPherron AC, Lee SJ: Suppression of body fat accumulation in myostatin-deficient mice. J Clin Invest 2002, 109:595–601

41. Farrell GC: Probing Prometheus: fat fueling the fire? Hepatology 2004, 40:1252–1255

42. Thevananther S: Adipose to the rescue: peripheral fat fuels liver regeneration. Hepatology 2010, 52:1875–1876